THE POTENTIAL OF MODERN SCIENCE

volume 3

London 2019

The Potential of Modern Science
volume 3

Editor: Babych Mykola Mykolayovich
Published by Sciemcee Publishing.
LP22772, 20-22 Wenlock Road
London, United Kingdom
N1 7GU
Sciemcee Publishing is part of SCIEMCEE.
It furthers the SCIEMCEE's mission by disseminating knowledge in the pursuit of education, learning and research at the highest international levels of excellence.

First Edition: 2019

A catalogue record for this publication is available from British Library.

ISBN 978-1-9993071-3-4
Includes bibliographical references and index.

SCIEMCEE
PUBLISHING LONDON

CONTENTS

Osadchuk A.V.
Doctor of Technical Sciences, Professor, Head of Radioengineering Department Vinnitsa National Technical Universit, Vinnitsa, Ukraine
Osadchuk V.S.
Doctor of Technical Sciences, Professor, Prof. of Radioengineering Department, Vinnitsa National Technical University, Vinnitsa, Ukraine
Osadchuk I.A.
PhD, Researcher of Radioengineering Department Vinnitsa National Technical University, Vinnitsa, Ukraine

MICROELECTRONIC FREQUENCY TRANSDUCERS OF THE MAGNETIC FIELD BASED ON SEMICONDUCTOR STRUCTURES WITH NEGATIVE DIFFERENTIAL RESISTANCE

Abstract. The work presents the results of the investigation of the main characteristics of self-excited oscillators based on two transistor structures with negative resistance and their expediency for constructing the transducers of a magnetic field with a frequency output signal is shown. A study was made of the magnetoreactive effect of primary magnetically sensitive elements, i.e. the dependence of the impedances of magnetoresistors, magnetodiodes, bipolar and field transistors on the effect of a magnetic field, which is the basis for the creation of magnetic field transducers with frequency output. Schemes of microelectronic frequency transducers of magnetic field in a wide frequency range from 10^3 to 10^7 Hz and sensitivity from 10^2 Hz/mT to 10^4 Hz/mT are proposed.

Keywords: frequency transducer; magnetic field; negative resistance; magnetically reactive effect.

Introduction

Magnetic field transducers are widely used in the automation and control of technological processes, environmental monitoring, monitoring of nuclear fusion parameters, in space technology, in scientific research, in medicine, in transport, etc. [1-3]. Currently, most magnetic field transducers are analog, in which the measured magnetic quantity is converted into voltage or current. This leads to measurement errors, loss of information in the channel between the output of the transducer and the input of the amplifying-conversion equipment, low powers of the output signal of transducers, their low noise immunity and speed. To eliminate the disadvantages of analog magnetic transducers, methods for constructing magnetic field frequency transducers based on autogenerator devices based on semiconductor structures with negative resistance are proposed. In such autogenerators, the magnetosensitive primary transducer is used additionally, as well as the active element of the circuit, which greatly simplifies the transducer circuits. It should be emphasized that until now, the influence of the magnetic field on the impedance characteristics of primary transducers and their subsequent influence on the frequency of the output signal of devices, the operating conditions of the transducers and their dependence on the direct and alternating voltages, their sensitivity and optimal operation regimes, have not been fully studied. The present paper is devoted to solving these problems.

Autogenerator - the main element of magnetic microelectronic frequency transducers

The oscillator of electric oscillations is the main element of the frequency transducers of the magnetic field, so the consideration of its operation in a broader context allows us to evaluate the dependence of the parameters of the transducers under the action of both external and internal factors. The appearance of semiconductor devices with decreasing volt-ampere characteristics (tunnel diodes, tunnel resonance diodes, Gunn diodes, avalanche diodes, lambda diodes, lambda transistors and a number of other devices) made it possible to use them not only as switches, amplifiers, threshold elements, and as a variety of sensory devices [4-7].

The basic scheme of the magnetic transducers, which realizes the current-voltage characteristic with a decreasing section, to which the negative resistance corresponds, is shown in Fig. 1.

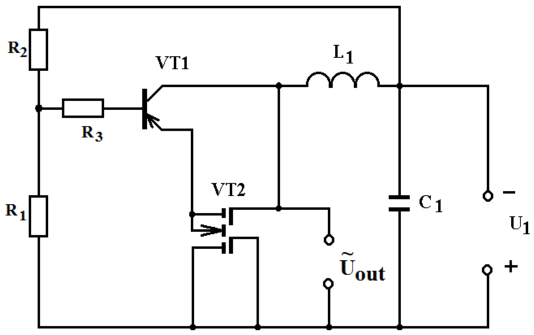

Figure 1. Schematic diagram of the oscillator

The circuit consists of bipolar and field-effect transistors, made in the form of a hybrid integrated circuit. The oscillatory circuit is formed by the external inductance L_1 and the capacitance C_1, as well as the internal capacitance of the transistors VT1 and VT2 with negative resistance at the electrodes of the gate-collector and the drain of the field-effect transistor. The constant voltage source U_1 is not necessary for the operation of the circuit, but with its help it is possible to vary within a wide range the value of the negative resistance, which facilitates the easy start of the generation of electrical signals in the transducer. One of the first studies devoted to the solution of the nonlinear oscillation equation was the work of Van der Pol [8]. In this paper, the equations of a parallel oscillatory circuit and a nonlinear volt-ampere characteristic were combined, which made it possible to obtain a second-order nonlinear differential equation. It can be solved numerically using modern computers. However, in practice, it is necessary to have analytical formulas for the amplitude of oscillations, amplitude and frequency sensitivity from changes in the external elements of the circuit, power regimes, therefore, quasi-linear analysis methods are used. In this case, the decreasing region of the current-voltage characteristic can be approximated by a piecewise-linear function or a polynomial of different orders, and the solution does not require complicated mathematical methods.

The physical processes that occur in the transducer circuit (Fig. 1) are quite complex, which does not give grounds for describing them by simple correct quantitative dependencies. Therefore, an analytical description of the static volt-ampere characteristic is based on its approximation by elementary functions. The most appropriate is the abstract approximation, which is not related to the physical processes in the transistor structure of the transducer, but relies primarily on its extreme points and the mathematical features of their vicinities. In Fig. 2 shows the static volt-ampere characteristic of the transducer circuit (Fig. 1).

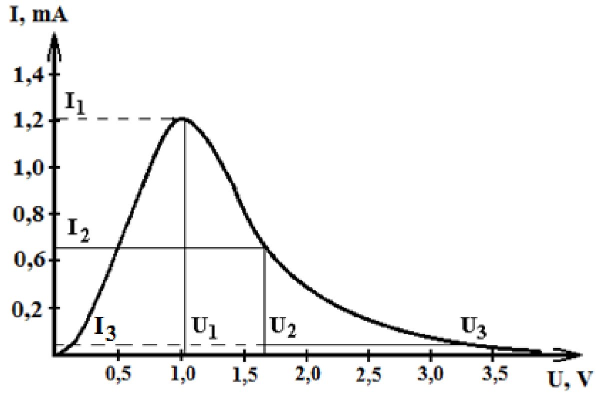

Figure 2. Static current-voltage characteristic of the transistor structure of the transducer

At the point of maximum (V_1, I_1) and a sufficiently small vicinity of it, the analytic expression of the static characteristic can be represented as a polynomial [9, 10]

$$I(U) = I_1 + a_1(U - U_1) + a_2(U - U_1)^2 + a_3(U - U_1)^3 + \dots\ , \tag{1}$$

where $a_1 = 0$ due to the necessary maximum condition $\left.\frac{dI}{dU}\right|_{U=U_1} = 0$, which causes inaccuracy of the linear description of the peak characteristic. The simplest nonlinear approximation is the parabolic approximation

$$I(U) = I_1 + a_2(U - U_1)^2, \tag{2}$$

which follows from equation (1). The branches of the parabola (Fig. 2), which have a common vertex (V_1, I_1), are asymmetric. The left branch is steeper and is described by expression

$$I = I_1\left[1 - \left(1 - U/U_1\right)^2\right], \tag{3}$$

which approximates the curve of the I-V characteristic of the structure for voltages $U \le U_1$. A more sloping right branch of the parabola passes through the point of intersection (U_2, I_2) and is described by equations in the voltages range $U_1 \le U \le U_2$

$$I = I_1 - \left(I_1 - I_2\right)\cdot\left(\frac{U - U_1}{U_2 - U_1}\right)^2. \tag{4}$$

The quadratic function does not very clearly describe the gently sloping minimum of the structure characteristic, so use a piecewise-power approximation [10]

$$I = I_3 + \left(I_2 - I_3\right)\cdot\left(\frac{U_3 - U}{U_3 - U_2}\right)^n \quad \text{at} \quad U_2 \le U \le U_3\ , \tag{5}$$

where n=2÷4. By varying the coefficient n in these boundaries, it is possible more accurately to describe the volt-ampere characteristic of the transistor structure of the transducer. Depending on the specific conditions of use, a simpler version of the decreasing region of the volt-ampere characteristic can be selected [10]

$$I = I_3 + (I_1 - I_3)\cdot\left(\frac{U_3 - U}{U_3 - U_1}\right)^n \quad \text{at} \quad U_1 \le U \le U_3 \ . \qquad (6)$$

Now we turn to the definition of the parameters of the self-oscillator, which in turn determines the main characteristics of the transducer, such as the conversion function, sensitivity, operating frequencies range, output voltage.

Calculation of the parameters of the self-oscillator is based on a quasilinear model. The electrical circuit of the self-oscillator is presented in general form in Fig.3

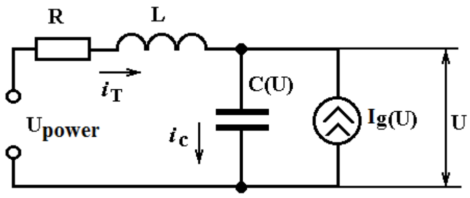

Figure 3. The electrical circuit of the oscillator

On the circuit, the total inductance $L = L_0 + L_1$ and resistance $R = r_0 + R_1$, where L_1, R_1 - inductance and resistance of the external circuit, L_0, r_0 – inductance and resistance of the terminals of the transistor structure, $C(U)$ - the capacitance of the transistor structure, which in general depends on the applied DC voltage, $I_g(U)$ is a current generator that simulates the behavior of negative resistance. The development of processes in this scheme is associated with a change in current i_T and voltage U. According to Fig. 3, the Kirchhoff equations become

$$U_{power} = i_T R + L\frac{di_T}{dt} + U \ , \qquad (7)$$

$$i_T = i_C + I(U) = C(U)\frac{dU}{dt} + I(U) \ . \qquad (8)$$

From equations (7) and (8) we find di_T/dt and dU/dt, hence

$$\frac{di_T}{dt} = \frac{U_{power} - i_T R - U}{L} \ , \qquad (9)$$

$$\frac{dU}{dt} = \frac{i_T - I(U)}{C(U)} \ . \qquad (10)$$

In a state of equilibrium, the (U_0, i_{T0}) currents and voltages do not change, so

$$\left.\frac{di_T}{dt}\right|_{i_T = i_{T0}} = 0 \ , \qquad \left.\frac{dU}{dt}\right|_{U=U_0} = 0 \ . \qquad (11)$$

Using conditions (11), from equations (9) and (10) we find

$$U_{power} - i_{T0} R - U_0 = 0 \ , \qquad (12)$$

$$i_{T0} - I(U_0) = 0 \ . \qquad (13)$$

The state of the circuit in accordance with (12) and (13) is realized at the points of intersection of the static volt-ampere characteristic and the static load line of the circuit

$$I(U_0) = (U_{power} - U_0) / R, \tag{14}$$

which is the equilibrium state of the circuit under study. To describe the operation of the circuit in the dynamic regime, we introduce new variables into equations (9) and (10), which have the form

$$u = U - U_0 \quad , \tag{15}$$

$$i = i_T - i_{T0} \quad , \tag{16}$$

The nonlinear static volt-ampere characteristic of the transistor structure near the equilibrium state is replaced by a linear function

$$I(U_0 + u) = I(U_0) + u / R_g , \tag{17}$$

where R_g is the differential resistance at the equilibrium point. The nonlinear capacitance of the transistor structure $C(U_0)$ at the collector-drain electrodes near the equilibrium state is assumed to be a constant that does not depend on the voltage. With these remarks, equations (9) and (10) are transformed into linear equations with constant coefficients:

$$\frac{di}{dt} = -\frac{Ri}{L} - \frac{u}{L} \quad , \tag{18}$$

$$\frac{du}{dt} = \frac{i}{C} - \frac{u}{R_g C} \quad . \tag{19}$$

To determine the characteristic equation on the basis of (18) and (19), it is necessary to differentiate with respect to time in Eq. (19).

$$\frac{d^2u}{dt^2} = \frac{di}{dt} \cdot \frac{1}{C} - \frac{1}{R_g C} \cdot \frac{du}{dt} \quad . \tag{20}$$

On the other hand, in accordance with the equivalent circuit of the self-oscillator (Fig. 3), one can write

$$i = i_c + i_g , \tag{21}$$

where $i_g = u / R_g$. Substituting (8), (9), (21) into (20), we obtain the equation

$$\frac{d^2u}{dt^2} + \frac{du}{dt}\left(\frac{R}{L} + \frac{1}{R_g C}\right) + \frac{u}{LC}\left(\frac{R}{R_g} + 1\right) = 0 \quad . \tag{22}$$

Starting from (22), the characteristic equation has the form

$$x^2 + x\left(\frac{R}{L} + \frac{1}{R_g C}\right) + \frac{1}{LC}\left(\frac{R}{R_g} + 1\right) = 0 \quad . \tag{23}$$

The roots of the characteristic equation are determined from the expression (23)

$$x_{1,2} = \frac{-\left(\frac{R}{L} + \frac{1}{R_g C}\right) \pm \sqrt{\left(\frac{R}{L} + \frac{1}{R_g C}\right)^2 - 4\frac{1}{LC}\left(\frac{R}{R_g} + 1\right)}}{2} \quad . \tag{24}$$

In accordance with Lyapunov's theory of stability, the roots of the characteristic equation (24) determine the equilibrium state of the system. If x_1 and x_2 have real values, then for $x_{1,2}<0$ any initial deviation in the system it will decay exponentially, and at $x_{1,2}>0$ - increase. If $x_{1,2}=a+jb$ (complex quantities), then in the system, sinusoidal oscillations are possible, and with $a>0$ oscillations increase, and with $a<0$ – damping. The solution of equation (22) has the form

$$
\begin{aligned}
u(t) = {} & A\exp\left[-\frac{1}{2}\left(\frac{R}{L}+\frac{1}{R_gC}\right)+\sqrt{\frac{1}{4}\left(\frac{1}{R_gC}+\frac{R}{L}\right)^2-\frac{1}{LC}\left(1+\frac{R}{R_g}\right)}\right]t+ \\
& +B\exp\left[-\frac{1}{2}\left(\frac{R}{L}+\frac{1}{R_gC}\right)-\sqrt{\frac{1}{4}\left(\frac{1}{R_gC}+\frac{R}{L}\right)^2-\frac{1}{LC}\left(1+\frac{R}{R_g}\right)}\right]t+\frac{U_{power}}{\left(1+R/R_g\right)}
\end{aligned}
\tag{25}
$$

where *A* and *B* are the coefficients that are determined from the initial conditions. The first two components of equation (25) describe a periodic process, the amplitude of which increases exponentially. The condition for the appearance of sinusoidal oscillations in the system is described by inequalities

$$\left(\frac{1}{R_gC}+\frac{R}{L}\right)<0 \quad , \tag{26}$$

$$\frac{1}{LC}\left(\frac{R}{R_g}+1\right)>0 \quad . \tag{27}$$

Combining (26) and (27), we obtain

$$\left(RC-\frac{L}{|R_g|}\right)^2-4LC<0 \quad . \tag{28}$$

Thus, the excitation of electric oscillations in the circuit (Fig. 3) at the resonant frequency will occur when conditions (28) are satisfied. The input impedance of the circuit is given by equation

$$Z=R+\frac{R_g}{\left(\omega CR_g\right)^2+1}+j\left(\omega L-\frac{\omega CR_g^2}{1+\left(\omega CR_g\right)^2}\right). \tag{29}$$

If condition

$$\omega L-\frac{\omega CR_g^2}{1+\left(\omega CR_g\right)^2}=0 \tag{30}$$

in the scheme comes a resonance. From the equation (30) we define the resonant frequency

$$\omega_p=\frac{1}{|R_g|C}\sqrt{\frac{R_g^2C}{L}-1} \quad . \tag{31}$$

If the frequency $\omega=\omega_p$ of the actual component of the input impedance is less than or equal to zero

$$R+\frac{R_g}{\left(\omega_pC_gR_g\right)^2+1}\le 0 \ , \tag{32}$$

then sinusoidal oscillations arise in the circuit.

The oscillation amplitude of the self-oscillator is determined on the basis of the energy balance: the energy that is absorbed by the oscillatory circuit of the self-oscillator should be equal to the energy that the negative resistance gives. The power that the negative resistance gives is determined by the expression

$$P_{NDR} = U_p I = U_p^2 / R_{NDR} \quad , \tag{33}$$

where U_p – the voltage at which the energy loss in the oscillatory circuit is compensated for by negative resistance, $I = U_p / R_{Loss}$ – the current in the parallel electrical circuit composed of the negative resistance and the loss resistance R_{Loss}. In steady-state mode, with a sinusoidal voltage P_{NDR} equal to the power loss P_{Loss}, which is consumed by the oscillatory circuit

$$P_{Loss} = \frac{1}{T}\int_0^T \frac{U^2}{R_{Loss}} dt = \frac{1}{T}\int_0^T \frac{U_m^2 \sin^2 \omega t}{R_{Loss}} dt = \frac{1}{2}\cdot\frac{U_m^2}{R_{Loss}} \quad . \tag{34}$$

Equating (33) and (34), we obtain

$$\frac{U_m^2}{2R_{Loss}} = \frac{U_p^2}{R_{Loss}}, \tag{35}$$

whence the amplitude of the voltage of the self-oscillator

$$U_m = \sqrt{2} U_p . \tag{36}$$

If the operating point moves along the decreasing section of the volt- ampere characteristic, then the voltage U_1 corresponds to a negative resistance R_{g1} a to the voltage $U_2 - R_{g2}$, which makes it possible to write the equation [8]

$$\frac{U_2}{U_1} = \frac{R_{g2}/R_{g1} - 1}{R_{g2}/R_{втр} - 1} \quad . \tag{37}$$

The amplitude sensitivity is determined from equation (37) taking into account the fact that, $U_p = U_2$ then

$$S_{R_{Loss}}^{U_m} = \frac{2R_{g2}}{R_{Loss}(R_{g2}/R_{Loss} - 1)} \quad . \tag{38}$$

Analysis of the expression (38) shows that the amplitude sensitivity of the self-oscillator increases as the R_{g2} values approach R_{Loss} however, on the other hand, this reduces the influence of higher harmonic components in the voltage of the self-oscillator. With a sinusoidal waveform, the resonance frequency can be represented in the form [8]

$$\omega_p = \left[1 - \frac{1}{4Q^2}\left(1 - \frac{R_{Loss}}{R_{g2}}\right)^2 \right]^{1/2} \quad . \tag{39}$$

where Q is the quality factor of the oscillatory circuit. On the basis of (39), the frequency sensitivity is determined relative to the change in the loss resistance [8]

$$S_{R_{Loss}}^{\omega_p} = \frac{1}{4Q^2}\left(1 - \frac{R_{Loss}}{R_{g2}}\right)^2 \quad . \tag{40}$$

The frequency is less, the smaller different the values of the resistances R_{g2} and R_{Loss} sensitivity. On the other hand, the value of the negative resistance must be such as to provide a self-excitation mode of the self-oscillator, which means that a small frequency sensitivity has a generator that operates near the stability limit. In Fig. 4 shows a volt-ampere characteristic of the transducer in static and dynamic conditions, which is obtained using curve tracer type Caltek CA-4810A.

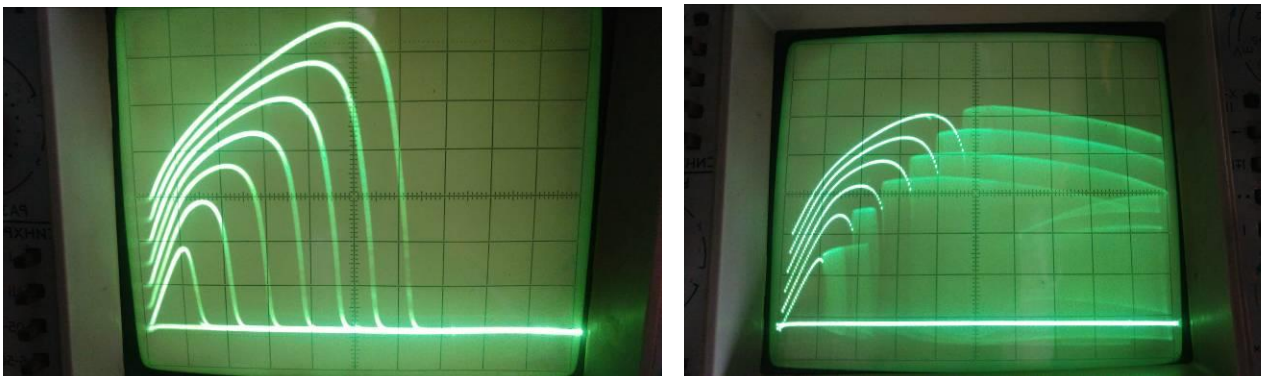

Figure 4. The volt-ampere characteristic of the transducer in static and dynamic modes

In Fig. 5 shows the theoretical and experimental dependences of the frequency of the transducer generation on the variation of the voltages U_1 and U_2.

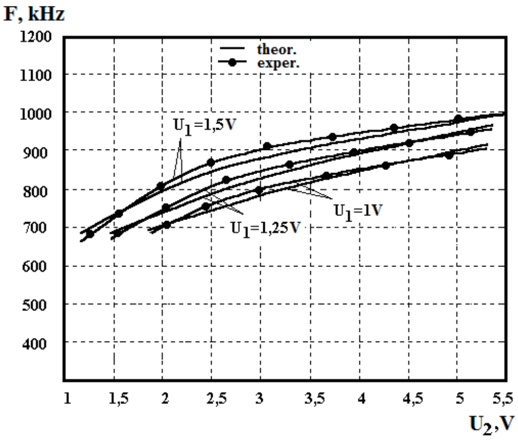

Figure 5. Theoretical and experimental dependences of the generation frequency on the supply voltage U_2

Elements of the theory of magnetoreactive effect in semiconductor devices

We understand dependence of the impedance of semiconductor devices on action of magnetic field as magnetoreactive effect. Magnetoresistors, point-contact diodes with long base, bipolar and field transistors belong to semiconductor devices which can be used as magnetosensing devices of frequency transducers. Why it is necessary to know theoretical dependences of impedances of above-mentioned semiconductor devices on action of magnetic field? The answer to this question lies in fundamental dependence of resonance frequency of the auto generator transducer on change active and reactive components of the impedance of magnetosensitive semiconductor devices, apparently of the formula (31). The active component of the impedance influences the negative resistance of the tune circuit, and the reactive component changes inductance or capacity of the tune circuit that leads to change of resonance frequency from influence of magnetic field. The impedance of magnetosensitive semiconductor devices, in turn, depends on change of the impedance of basic region of devices where there is the interaction of magnetic field to the electrons or holes moving in this region. Thus, it is necessary to know the impedance of basic area of magnetosensitive semiconductor devices from action of magnetic field. It is possible to solve these problems or on the basis of consideration of the fundamental equation of transfer of charge carriers in semiconductor devices, or proceeding from equivalent circuits of these devices. The second way is more practical in connection with use of modern computers though the solution of the equation of transfer for diodes and transistors shows what parameters of devices most strongly depend on action of magnetic field [7].

Let's pass to consideration of dependence of resistance of the magnetoresistor on action of magnetic field. The magnetosensitive semiconductor resistor consists of the magneto-resistive element which is located in air gap of controlling magnetic field. Operation of such resistors is based on use of the magnetoresistance effect which leads to increase in resistance of the resistive element at action on it magnetic field. The magneto-resistive element or the magnetoresistor is characterized by the rated resistance of R_0 in the absence of magnetic field, of relation resistance in cross magnetic field with the defined value of induction (0,5 or 1 T) to rated value R_B / R_0, TKR – the temperature coefficient of resistance. The main characteristic of the magnetoresistor is the dependence of its resistance on the value of induction of magnetic field which affects it.

The rated resistance of the magnetoresistor is defined by electric conductance of semiconductor material which is used for its preparation and design data. Increase in resistance during action of magnetic field is caused by action of Lorentz force that leads to deformation of streamlines. Relative change of unit resistance of semiconductors with one type of charge carriers taking into account statistical dispersion of their speeds in weaker cross magnetic field ($\mu_n B \ll 1$) is defined by the formula [11]

$$\frac{\Delta\rho}{\rho_0} = \frac{4-\pi}{\pi}\left(\frac{3\pi}{8}\right)(\mu_n B)^2, \tag{41}$$

where $\Delta\rho = \rho_B - \rho_0$; ρ_B, ρ_0 – respectively the unit resistance of the semiconductor in magnetic field with induction B and for lack of magnetic field. Taking into account two types of charge carriers in material n – like conductivity [11]

$$\frac{\Delta\rho}{\rho_0} = \left(\frac{3\pi}{8}\right)^2 B^2 \left[\frac{4}{\pi}\cdot\frac{\mu_n^3 n + \mu_p^3 p}{\mu_n n + \mu_p p} - \left(\frac{\mu_n^2 n - \mu_p^2 p}{\mu_n n - \mu_p p}\right)^2\right] \tag{42}$$

where μ_n, μ_p – respectively mobility of electrons and holes, n, p –concentration of electrons and holes. The maximum of the magnetoresistive effect is reached with such ratio of electrons and holes [11]

$$\frac{n}{p}=\left[\frac{4}{\pi}\left(1-\frac{1}{b}\right)+\frac{2}{b}\right]\Bigg/\left[\frac{4}{\pi}(1-b)+2b\right], \tag{43}$$

where $b=\mu_n/\mu_p$, at the same time

$$\frac{\Delta\rho}{\rho_0}=\left(\frac{3\pi}{8}\right)^2 B^2\left(\mu_n\mu_p+\frac{\mu_n-\mu_p}{\pi}\right)\frac{4}{\pi}.$$

Upon transition from weak magnetic fields to strong, the law of change of unit resistance from the value of magnetic induction gradually changes from square to linear. Change of resistance which is caused by deformation of streamlines at action of magnetic field depends on its geometrical sizes, electrical properties of the semiconductor and value of magnetic induction. The greatest change of resistance at action of magnetic field is observed at the disk magneto-resistive element with contacts in the center and the periphery of the disk. In weaker magnetic field change of its resistance is described by the formula [11]

$$\frac{R_B}{R_0}=\frac{\rho_B}{\rho_0}\left(1+(\mu_n B)^2\right). \tag{44}$$

However in practice the quared magneto-resistive elements received the greatest spread. For ensuring high sensitivity to magnetic field the design has to answer the condition

$$\frac{l}{W}<<1, \tag{45}$$

where l – length of the site of the magneto-resistive element between equipotential contacts, W – width of the magneto-resistive element. Change of resistance of the squared magneto-resistive element in weaker cross magnetic field if conditions are satisfied $\mu_n B\le 0{,}45$ and $l/W\le 0{,}35$, with an accuracy of one percent it is possible to calculate by the formula [11]

$$\frac{R_B}{R_0}=\frac{\rho_B}{\rho_0}\left(1+(\mu_n B)^2\left(1-0{,}54\frac{l}{W}\right)\right). \tag{46}$$

In case of strong magnetic fields when Hall's corner comes nearer to $\pi/2$, for calculation of change of resistance of the magneto-resistive element when performing the condition $l<<W$ the formula is used [11]

$$\frac{R_B}{R_0}=\frac{\rho_B}{\rho_0}\left(1+\frac{W}{l}\mu_n B_1-\frac{4}{\pi}\ln 2\right). \tag{47}$$

As for magneto-resistive elements are known rated resistance R_0, resistance at rated value of induction R_{B1} and also value of induction B_2 in transition point from change of resistance, square to the linear law, dependence $R=f(B)$ it is possible to approximate such expressions: in the region of weak magnetic fields [11]

$$R_B=R_0(1+\beta B^2), \tag{48}$$

and in the region of strong magnetic fields

$$R_B=R_0+(R_{B1}-R_0)\frac{2B-B_2}{2B_1-B_2}, \tag{49}$$

where
$$\beta=\frac{R_{B1}-R_0}{R_0(2B_1B_2-B_2^2)}.$$

Let's consider dependence of the impedance of basic area of the point-contact diode on magnetic induction. In practice as magnetodiodes point-contact diodes with long base when length of basic area is more than diffusion length of charge carriers are used. In such diodes the forward current is defined by nonequilibrium conductivity of basic area. Distribution of carriers in basic area depends on mobility and the lifetime of charge carriers. In magnetic field owing to the magnetoresistance the mobility of carriers of current decreases that leads to reduction of conductivity of the diode. The magnetosensitivity of long-base diodes many times over exceeds magnetosensitivity of magnetoresistors. Magnetic field in magnetodiodes not only reduces mobility, but also bends streamlines. In long diodes Hall's field is absent as a result of almost identical electron concentration and holes. Streamlines are extended that leads to reduction of depth of penetration of the injected charge carriers and additional reduction of conductivity modulation of base, and it, in turn, leads to increase in magnetosensitivity of diodes.

The curvature of streamlines increases concentration of charge carriers at one edge of basic area and lowers at another. Redistribution of charge carriers raises the role of the surface recombination, and it, in turn, leads to change of the lifetime of charge carriers. If recombination rates on edges are identical, then the lifetime decreases and current of such magnetodiode decreases at action of magnetic field.

The impedance of basic area of the point-contact diode which is consistently connected to the junction p-n impedance is received in work of J. Ladany [12]. Calculation of the impedance is accomlished on the basis of the joint solution of the equation of continuity and the equation of electric field in basic area of the diode working at the high level of injection. The impedance of basic area is described by expression [12]

$$Z = \frac{W}{A\sigma}(b+1)e^{-qU_0/2kT} + j\omega\left[\frac{W}{A\sigma}\frac{W^2}{2D'}e^{-qU_0/2kT}\left(\frac{qU_0}{kT} - \frac{2}{3}(b+1) - \frac{1}{2}\right)\right], \quad (50)$$

where W, A, σ – thickness of basic area, its square and conductivity, respectively b – relation of mobility of electrons towards holes mobility, q – electron charge, U_0 – voltage drop on basic area, k – Boltzmann constant, T – temperature in Kelvins, D' – coefficient of ambipolar diffusion. Thus, the equivalent circuit of the long diode can be presented in the form

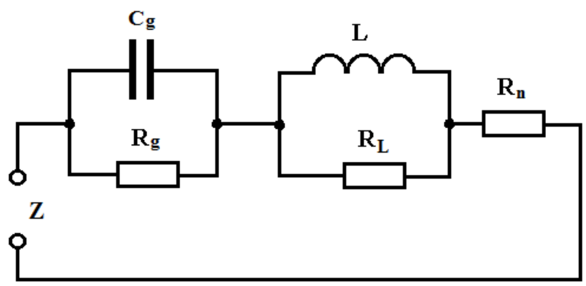

Figure 6. Equivalent circuit of the long diode: C_g – diffusion capacity of p-n junction, R_g – resistance of emitter junction, L – inductance of basic area, R_L – resistance of basic inductance, R_n – resistance of the passive part of the basic area

Taking into account the magnetoresistance at action of magnetic field it is possible to record dependence of elements of the equivalent circuit (fig. 6) on magnetic induction at small magnetic fields with the diode

$$R_g(B) = \frac{kT}{qI_E}\left[1+(\mu_p B)^2\right], \tag{51}$$

where I_E – emitter junction current, μ_p – holes mobility, B – magnetic induction.

$$C_g(B) = \left(\frac{W^2}{2D'}\right) \Big/ \frac{kT}{qI_E}\left[1+(\mu_p B)^2\right]. \tag{52}$$

The dependence of inductance of basic area on magnetic induction is described by expression

$$L(B) = \frac{W}{A\sigma}\left(\frac{W^2}{2D'}\right)\exp\left(-\frac{qU_0}{2kT}\left(\frac{qU_0}{kT} - \frac{2}{3}(b+1) - \frac{1}{2}\right)\left(1+(\mu_p B)^2\right)\right). \tag{53}$$

Inductance resistance from magnetic induction has the appearance

$$R_L(B) = \frac{W(b+1)}{A\sigma}\exp\left(-\frac{qU_0}{2kT}\left(1+(\mu_p B)^2\right)\right). \tag{54}$$

Resistance of the passive part of the basic area is described by the formula

$$R_P(B) = R_{P0}\left(1+(\mu_p B)^2\right). \tag{55}$$

where R_{P0} – resistance of the passive part of the basic area without action of magnetic field.

The impedance of the long point-contact diode on the basis of the equivalent circuit (fig. 6) is described by expression

$$Z = \left[\frac{R_g}{1+(\omega C_g R_g)^2} + \frac{R_L(\omega L)^2}{R_L^2+(\omega L)^2} + R_P\right] + j\omega\left[\frac{LR_L^2}{R_L^2+(\omega L)^2} - \frac{R_g^2 C_g}{1+(\omega C_g R_g)^2}\right]. \tag{56}$$

On the basis of (56), and considering (51)-(55), dependences of active and reactive components of the impedance of the diode on magnetic induction are calculated. The dependence of the active and reactive components of the impedance on magnetic induction is presented on fig. 7.

Apparently from fig. 7, the absolute sensitivity from magnetic induction for the active component is equal $17{,}2\,\mathrm{Om/mT}$, and for the reactive component $-22{,}6\,\mathrm{Om/mT}$, what confirms the possibility of use of magnetoreactive effects for creation of transducers of magnetic field in the frequency output signal.

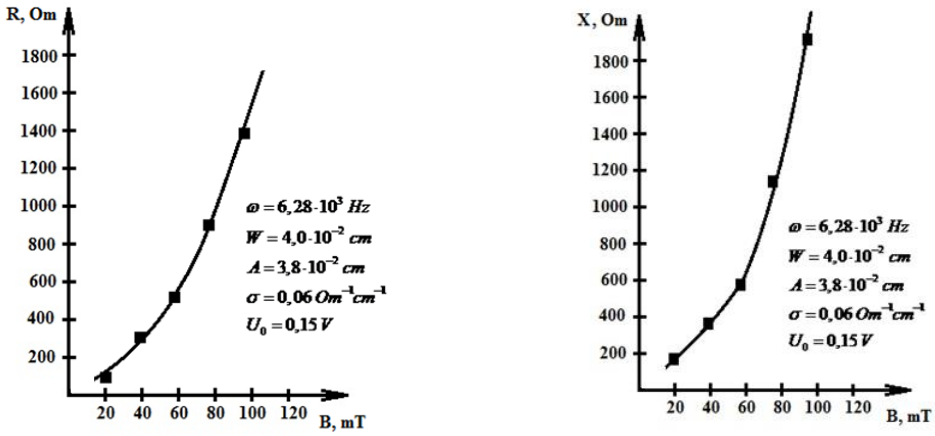

Figure 7. Dependence of the active and reactive components of the impedance of the long diode on magnetic induction.

Analytical expression for the impedance of basic area of bipolar transistors at high levels of injection is received in work [13]

$$Z_B = \frac{kT}{qI_E} \cdot \frac{2}{(b+1)}\left[1 + \frac{j\omega L_E / r_1}{1 + j\omega(L_B / r_2)}\right], \tag{57}$$

where
$$L_B = r_1 \frac{W^2}{2D'}\left(\frac{qU_0}{kT} - 1\right), \tag{58}$$

$$r_1 = \frac{2}{b+1} \cdot \frac{kT}{qI_E}, \quad r_2 = r_1\left(\frac{qU_0}{kT} - 1\right), \tag{59}$$

L_B – inductance of basic area, r_2 – inductance resistance L_B, r_1 – emitter resistance, U_0 – voltage drop on basic area at the high level of injection, I_E – emitter current. Division of expression (57) into the valid and imaginary parts leads to the look

$$Z_B = r_1 + \frac{r_2\omega^2 L_B^2}{r_2^2 + (\omega L_B)^2} + j\omega\frac{L_B r_2^2}{r_2^2 + (\omega L_B)^2}. \tag{60}$$

According to expression (60) the equivalent circuit of basic area of the bipolar transistor has the appearance [13]

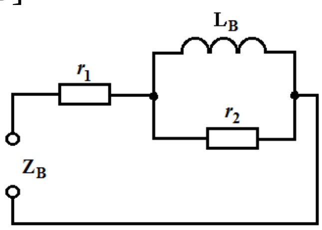

Figure 8. Eequivalent circuit of basic area of the bipolar transistor.

According to the magnetoresistance of dependence of elements of the equivalent circuit (fig. 10) on action of magnetic field it is possible to present in such form

$$r_1(B) = r_{01}\left(1 + (\mu_p B)^2\right), \tag{61}$$

$$r_2(B) = r_{02}\left(1 + (\mu_p B)^2\right), \tag{62}$$

$$L_B(B) = r_{01}\left(1 + (\mu_p B)^2\right)\left(\frac{W^2}{2D'}\right)\left(\frac{qU_0}{kT} - 1\right), \tag{63}$$

where r_{01}, r_{02} – emitter resistance and inductance without action of magnetic field.

Calculated dependences of active and reactive components of the impedance of basic area of the bipolar transistor on magnetic induction are presented on fig. 9, according to expression (60). The analysis of curve fig. 9 shows that the absolute sensitivity of the active component from magnetic induction is 13,5 Om/mT, and reactive – 0,16 Om/mT that is quite acceptable for creation of frequency magnetic transducers on bipolar magnetosensitive transistors. As numerical estimations show in weak magnetic fields the main contribution to magnetosensitivity of bipolar transistors gives change of effective length of basic region [14].

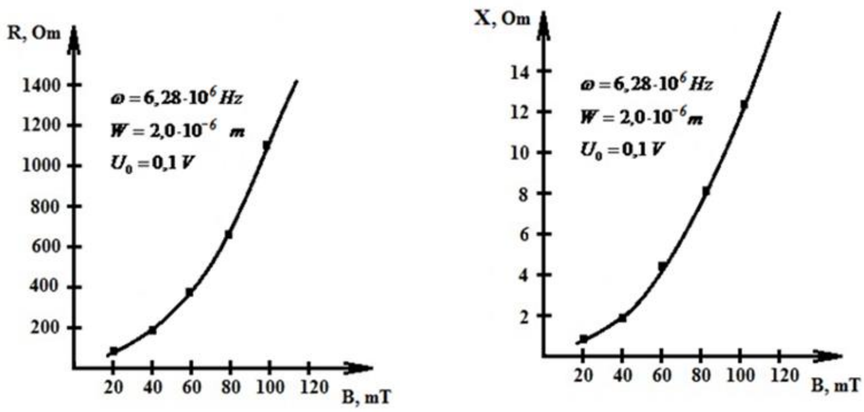

Figure 9. Dependence of the active and reactive components of the impedance of basic area of the bipolar transistor on magnetic induction.

Let's estimate magnetosensitivity of the impedance of field transistors. At action of magnetic field on the field effect transistor channel there is the magnitorezistivny effect which results in dependence of current of the channel on magnetic induction. Cross magnetic field with the magnetic displacement vector $+B$ rejects electrons on the way to the drain to subbarrier dielectric, and at action of the magnetic displacement vector in the opposite direction – deep into the volume of the semiconductor substrate (fig. 10).

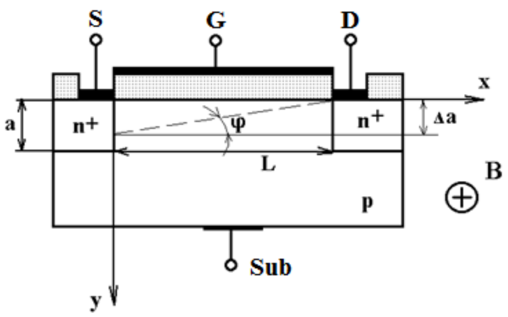

Figure 10. Structure of the magnetosensitive field-effect transistor.

According to fig. 10, it is possible to write down

$$I_{DS} = A\sigma E_X , \tag{64}$$

where A – the area of the channel, σ – conductivity of the channel, E_x – electric field intensity in the channel, I_{DS} – current via the channel. If the channel is affected by cross magnetic field, then current via the channel is described by the formula

$$I_{DS} = AE_X \cdot \sigma', \tag{65}$$

where σ' – conductivity of the channel at action of magnetic field. Relative change of conductivity of the field effect transistor channel has the form

$$\frac{\sigma - \sigma'}{\sigma} = \frac{\mu_n^2 B^2}{2}, \tag{66}$$

then taking into account (64), (65) and (66) it is possible to write down

$$I_{DS} - I'_{DS} = I_{DS} \cdot \left(\frac{\mu_n^2 B^2}{2} \right) \tag{67}$$

from where

$$I'_{DS} = I_{DS} \cdot \left(1 - \frac{\mu_n^2 B^2}{2} \right). \tag{68}$$

The drain current of the field transistor in linear area of the volt-ampere characteristic is defined by the equation [14]

$$I_{DS} = \frac{Z\mu_n C_0}{L} \cdot \left[(U_G - U_T) U_{DS} - \frac{1}{2} U^2{}_{DS} \right] \tag{69}$$

where Z – width of the channel, L – length of the channel, μ_n – mobility of electrons in the channel, W_0 – the capacity of subbarrier dielectric per acre, U_G – voltage on the drain concerning the source, U_{DS} – voltage on the drain concerning the source, U_T – threshold voltage.

Taking into account action of magnetic field, according to (68) and (69), it is possible to write down

$$I'_{DS} = \frac{Z\mu_n C_0}{L} \cdot \left[(U_G - U_T) U_{DS} - \frac{1}{2} U^2{}_{DS} \right] \cdot \left(1 - \frac{\mu_n^2 B^2}{2} \right) \tag{70}$$

In the field of saturation the drain current taking into account (68) is described by the formula

$$I'_{DS_{Sat}} = \frac{Z\mu_n \cdot C_0}{2L} \cdot (U_G - U_T)^2 \cdot \left(1 - \frac{\mu_n^2 B^2}{2} \right). \tag{71}$$

Thus, for obtaining analytical dependence of the active and reactive component on magnetic induction taking into account (70) and (71) it is necessary to define the impedance on electrodes the magnetotransistor source- drain on the basis of the nonlinear equivalent circuit [15]. Parameters of elements of the equivalent circuit for calculation of the impedance are taken from work [16]. Dependences of the active and reactive component of the impedance of the field transistor on magnetic induction are presented on fig. 11.

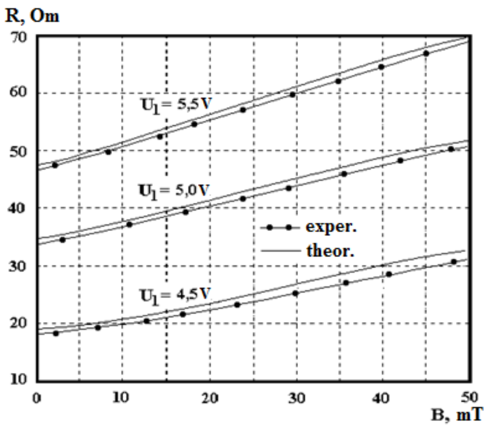

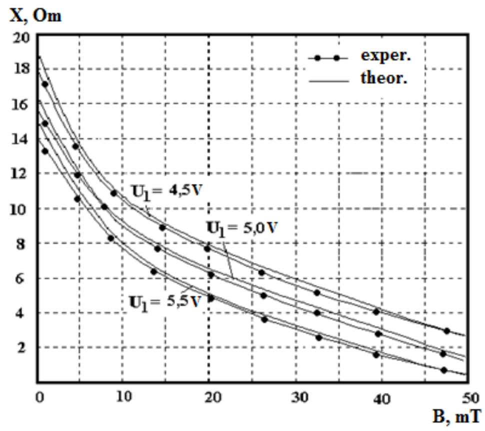

Figure 11. Dependence of the active and reactive components of the impedance of the field effect transistor on magnetic induction

The analysis of curves in fig. 11 shows that absolute sensitivity of the active component from magnetic induction of the accounts for 0.3 Om/mT, and on the reactive component 0.28 Om/mT what allows to use field transistors as magnetosensing devices in transducers with the frequency output signal.

Microelectronic frequency transducers of magnetic field

The scheme of the magnetic microelectronic frequency transducer is presented on fig. 12. It consists of two complementary field transistors, and the feedback circuit of VT1 and VT2 transistors included the magnetosensitive resistance of R_1which magnetic field affects [17].

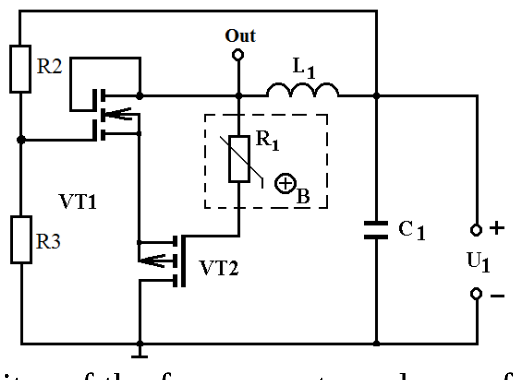

Figure 12. The circuitry of the frequency transducer of magnetic field with the magnetoresistor

The tuned circuit of the transducer is formed by inductance of L, extrinsic capacitance C_1 and internal capacity on electrodes the drain-drain of VT1 and VT2 transistors. Losses of energy in the tuned circuit are offset due to energy of negative resistance which is defined by the choice of the working point on the falling-down site of the volt-ampere characteristic of the scheme. The equivalent circuit of the transducer on alternating current is presented on fig. 13.

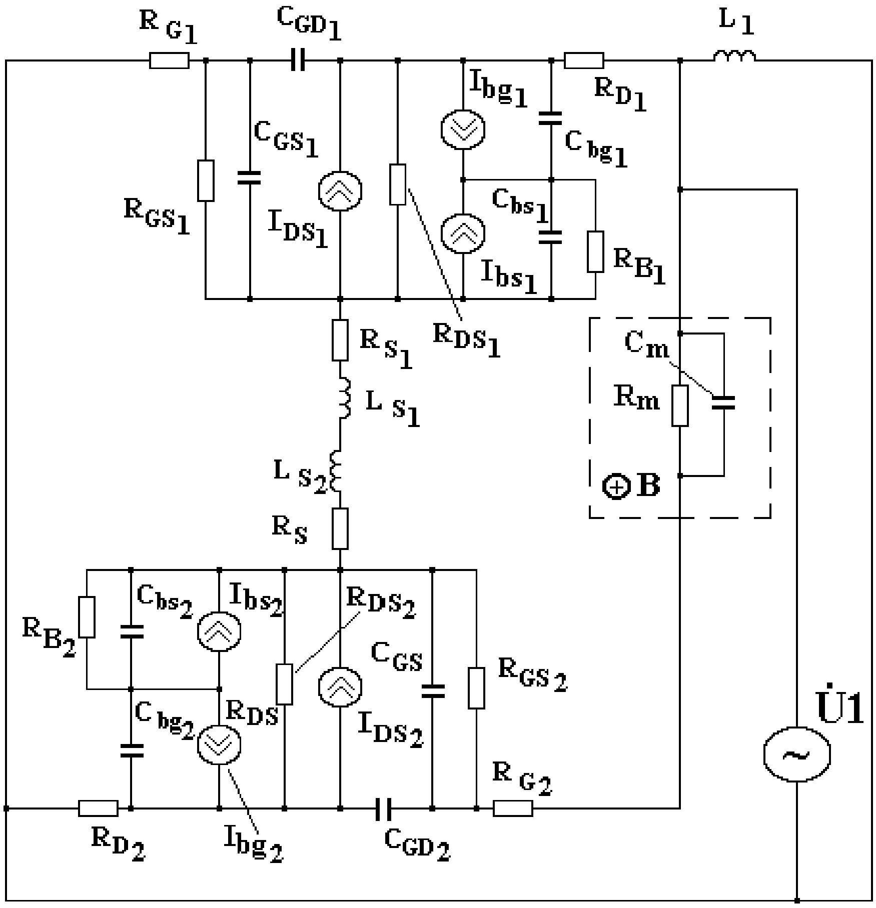

Figure 13. The equivalent circuit of the transducer of magnetic field on the basis of the magnetoresistor on alternating current

By means of constant voltage sources of U_1 and U_2 the working point of the self-oscillator is chosen on the falling-down site of the volt-ampere characteristic. It corresponds to steady generation of electric fluctuations. At action of magnetic field on the magnetoresistor of R_1 there is voltage variation which shifts the working point of the transducer on the falling-down site of the volt-ampere characteristic. It is equivalent to change of active and reactive components, output impedance of the device that, in turn, leads to change of resonance frequency. Output impedance of the device (fig. 13) is calculated on the basis of Kirchhoff's equations according to the chosen loop currents in the transformed equivalent circuit. The decision of the equations of Kirchhoff is calculated on PC by Gauss's method by means of the Matlab 7.11 program [18]. The value of parameters of the equivalent circuit (fig. 13) for analytical calculations is taken from works [15,16].

For experimental studies the hybrid integrated circuit was manufactured. In this scheme the field transistors BSS284 and BF998 were used. Dependences of active and reactive components of output impedance of the transducer on magnetic induction are presented on fig. 14.

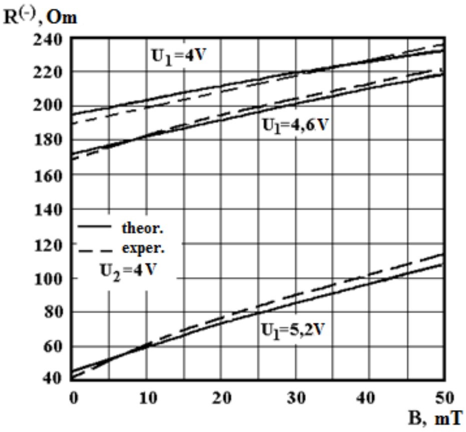

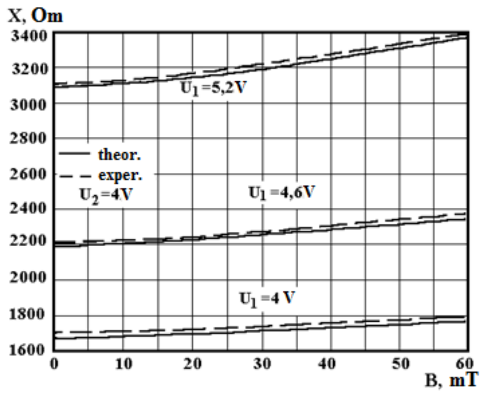

Figure 14. Schedules of theoretical and experimental dependences of the active and reactive components of the impedance of the transducer on magnetic induction

Apparently from the schedule (fig. 14), the active component of output impedance of the magnetic transducer increases with increase in induction of magnetic field that is connected with change in resistance of the magnetosensitive element. The dependence of the reactive component of output impedance of the magnetic transducer (fig. 14) increases with increase in magnetic induction that is explained because of reduction of equivalent capacity of the tuned circuit. Theoretical and experimental dependences of function of transformation (generation frequency) on magnetic induction are presented on fig. 15. At action of magnetic field on magnetoresistor the frequency of generation increases, so at value of magnetic induction 10 mT the frequency of generation was 1572 kHz, and at 60 mT it increased on 30 kHz. It is experimentally established that the choice of the regime on the direct current gives the chance to receive almost linear relation of function of transformation from magnetic induction.

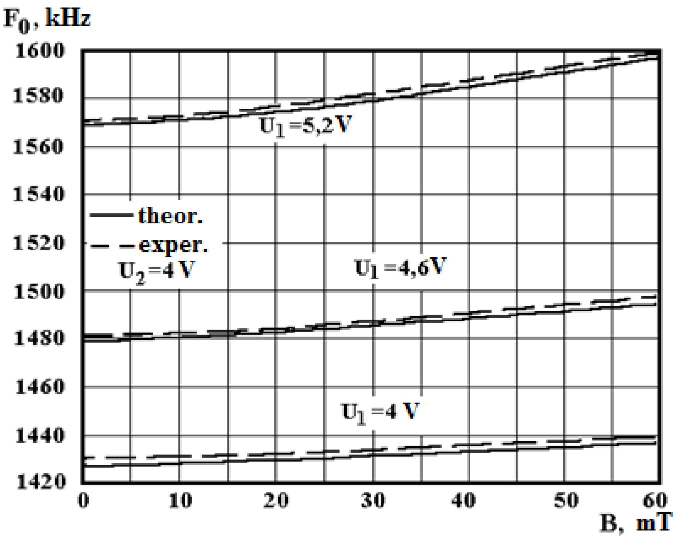

Figure 15. Schedules of theoretical and experimental dependences of function of transformation on magnetic induction

Function of transformation is defined by expression

$$F_0 = \frac{\sqrt{2}\sqrt{\dfrac{R_m^2(B)C_{GD1}C_m + R_m^2(B)C_m^2 - LC_{GD1} - A_1}{LC_{GD1}R_m^2(B)C_m^2}}}{4\pi}, \qquad (72)$$

where $A_1 = \sqrt{(R_m^2(B)C_m^2 + C_{GD1}R_m^2(B)C_m - LC_{GD1})^2 + 4LC_{GD1}R_m^2(B)C_m^2}$.

The sensitivity of the transducer is defined on the basis of (72)

$$S_B = -\frac{1}{4}\frac{\sqrt{2}\left(\dfrac{\partial R_m(B)}{\partial B}\right)\left(-R_m^2(B)C_{GD1}C_m + R_m^2(B)C_m^2 - \sqrt{A_2} + LC_{GD1}\right)}{\pi R_m^3(B)C_m^2\sqrt{A_2}\sqrt{\dfrac{R_m^2(B)C_mC_{GD1} + R_m^2(B)C_m^2 + \sqrt{A_2} - LC_{GD1}}{LC_{GD1}R_m^2(B)C_m^2}}}, \qquad (73)$$

where $A_2 = R_m^4(B)C_m^2C_{GD1}^2 + 2R_m^4(B)C_m^3C_{GD1} - 2LC_{GD1}^2R_m^2(B)C_m + R_m^4(B)C_m^4 + 2LC_{GD1}R_m^2(B)C_m + L^2C_{GD1}^2$.

Apparently from fig. 16, the sensitivity of the magnetic frequency transducer is 800 Hz/mT at the operating frequency of 1592 kHz at the temperature of 20 ^{0}C. As shows experimental studies, the optimum value of supply voltage is 4.6 V at which the smallest frequency change of generation at change of temperature from 20 ^{0}C to 80 ^{0}C is observed. In the region of temperatures from 20 ^{0}C to 50 ^{0}C the most temperature and stable operation of the transducer takes place.

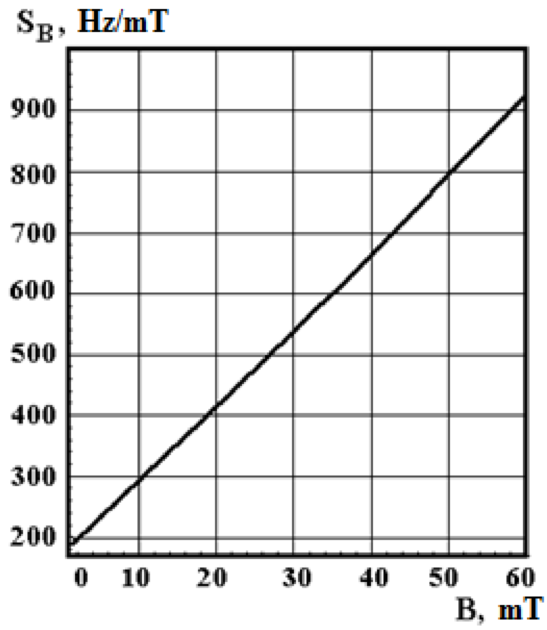

Figure 16. Schedule of rated dependence of sensitivity of the transducer

The electrical circuit of the microelectronic frequency transducer with the magnetosensitive diode is shown in fig. 17. It represents the hybrid integrated circuit which consists of two bipolar transistors with different types of conductivity that is the condition of creation of the auto generator converting device, in the positive feedback circuit switched on the magnetosensitive diode [19]

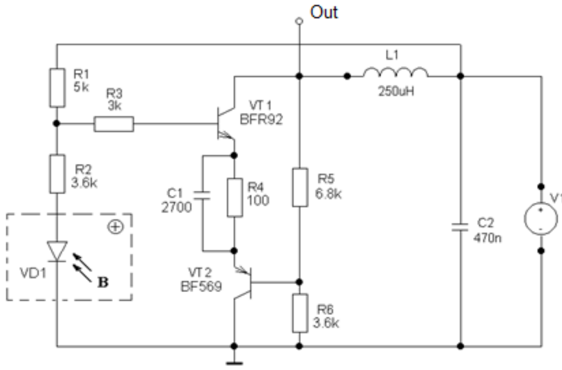

Figure 17. The electrical circuit of the transducer of magnetic field magnetosensitive diode

On electrodes the collector of VT1 and VT2 transistors exists the impedance which active component has negative value, and reactive capacity character. The tuned circuit is created through connection of inductance L_1 with the collector of VT1 and consistently with inductance of capacity C_2. Losses of energy in the tune circuit are offset by energy of negative resistance. At action of magnetic field on the magnetosensitive diode there is the change of active and reactive components of output impedance of the transducer that leads to frequency change of generation of the device. The equivalent circuit of the frequency transducer of magnetic field is presented on fig. 18.

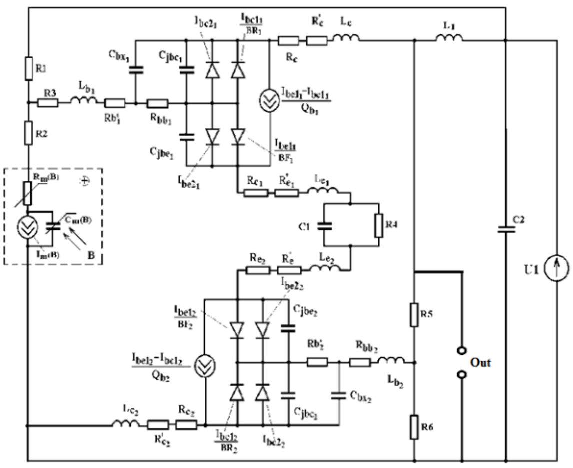

Figure 18. The equivalent circuit of the frequency transducer of magnetic field with the magnetosensitive diode

On the basis of this scheme the function of transformation of the device proceeding from the equality condition to zero reactive component at the resonance frequency is defined. Analytical expression of function of transformation has the form

$$F_0 = \frac{1}{2\pi}\left[\frac{-\left(A_1 - D_1\right) + \sqrt{\left(A_1 - D_1\right)^2 + 8(C_{jbe} + C_{bx})G_1}}{2G_1}\right]^{1/2}, \tag{74}$$

where $A_1 = L_1 C_{bx} C_{jbe} - (C_{jbe} + C_{bx})\left[C_m(B) R_m(B)\right]^2$; $D_1 = R_m^2(B) C_m(B) C_{jbe} C_{bx}$. $G_1 = L_1 C_{bx} C_{jbe} C_m^2(B) R_m^2(B)$.

The graphic dependence of function of transformation, i.e., dependence of frequency of generation of the transducer on magnetic induction, is presented on fig. 19.

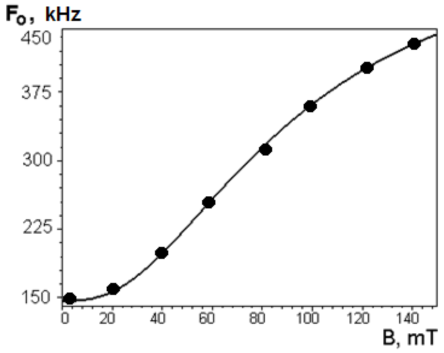

Figure 19. Schedule of experimental dependence of function transformation on magnetic induction

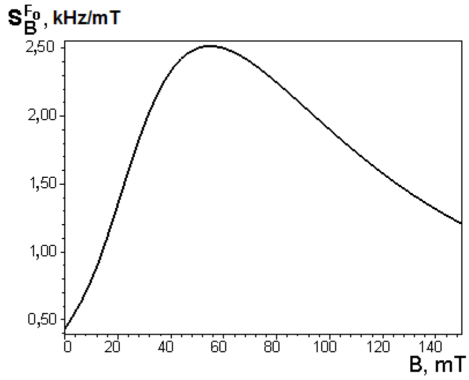

Figure 20. Schedule of rated dependence of sensitivity of the transducer

The sensitivity of the transducer is defined on the basis of expression (74) and is described by the equation

$$S_B^{F_0}=\frac{1}{8}\Bigg(2(C_{jbe}+C_{bx}C_m^2(B)R_m(B)\left(\frac{\partial R_m(B)}{\partial B}\right)+2R_m(B)C_m(B)C_{jbe}C_{bx}\left(\frac{\partial R_m(B)}{\partial B}\right)+\frac{1}{2}\big(2(A_1-$$
$$-D_1)\Big(-2(C_{jbe}+C_{bx})\times C_m^2(B)R_m(B)\left(\frac{\partial R_m(B)}{\partial B}\right)--2R_m(B)C_m(B)C_{jbe}C_{bx}\left(\frac{\partial R_m(B)}{\partial B}\right)\Big)+$$
$$+24(C_{jbe}+C_{bx})L_1C_{jbe}C_{bx}C_m^2(B)R_m(B)\left(\frac{\partial R_m(B)}{\partial B}\right)\Big)\Big/\sqrt{(A_1-D_1)^2+12Y_1}-\Big)\Big/\pi L_1C_{jbe}C_{bx}\times \qquad (75)$$
$$\times C_m^2(B)R_m(B)-\frac{1}{4}\Big(\Big(-A_1+D_1+\sqrt{(A_1-D_1)^2+12Y_1}\Big)\left(\frac{\partial R_m(B)}{\partial B}\right)\Big)\Big/\big(\pi L_1C_{jbe}C_{bx}C_m^2(B)R_m^3(B)\big),$$

where $Y_1=(C_{jbe}+C_{bx})L_1C_{jbe}C_{bx}C_m^2(B)R_m^2(B)$.

The schedule of sensitivity of the transducer is presented on fig. 20. Apparently from the schedule, the greatest sensitivity of the device lies in the range of 35-90 mT, and 2-2.5 kHz/mT make.

The circuit of magnetic transducer is shown in Fig. 21. Magnetosensitive bipolar transistor VT1 and MOS transistor VT2, make up a generator of electrical oscillations, in which the oscillating circuit is formed by the capacitive component of the impedance with a negative value of active component of the electrodes collector-drain transistors VT1, VT2 and inductance L1.

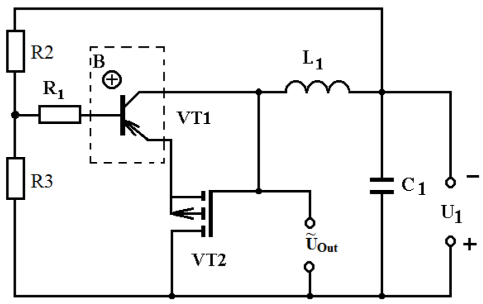

Figure 21.Circuit of radio measuring magnetic transducer based on bipolar and field-effect transistors

Thus, under the influence of magnetic field on the magnetosensitive bipolar transistor VT1 both the capacitance of the tuned circuit and the value of the negative resistance are changed, that leads to the change the resonance frequency of the oscillator [20]. Bipolar transistor, which is a magnetosensitive element, is switched in the circuit with common emitter, which ensures its better sensitivity to the magnetic field in comparison with the circuit with a common base. During the action of a magnetic cross field on the base region of the bipolar transistor occurs the bend of the trajectory of the injected charge carriers. This is equivalent to the fact that the magnetic field increases the effective length of the base W and mobility at the same time remains steady.

Figure 22 presents theoretical and experimental dependences of generation frequency on the magnetic induction. Under the influence of magnetic field on the magnetosensitive transistor oscillation frequency decreases, so at the value of magnetic induction 10 mT oscillation frequency was 1458 kHz and at 50 mT it was decreased to 103 kHz. It was established experimentally that the choice of dc power mode makes it possible to obtain almost linear dependence of the transfer function on the magnetic induction. The conversion function is described by the equation

$$F_0 = \frac{1}{2}\frac{\sqrt{\dfrac{C_{be}(B)C_1 + C_{bc}(B)C_1 + C_{be}(B)C_{bc}(B)}{LC_{bc}(B)C_{be}(B)C_1}}}{\pi}\ . \tag{76}$$

Magnetic sensitivity of the transducer is determined based on the equation (76)

$$\begin{aligned} S_B = \frac{1}{4}\Bigg(& \frac{\left(\dfrac{\partial C_{be}(B)}{\partial B}\right)C_1}{LC_{bc}(B)C_{be}(B)C_1} + \frac{\left(\dfrac{\partial C_{bc}(B)}{\partial B}\right)C_1}{LC_{bc}(B)C_{be}(B)C_1} + \frac{\left(\dfrac{\partial C_{be}(B)}{\partial B}\right)C_{bc}(B) + \left(\dfrac{\partial C_{bc}(B)}{\partial B}\right)C_{be}(B)}{LC_{bc}(B)C_{be}(B)C_1} - \\ & - \frac{A_1\left(\dfrac{\partial C_{bc}(B)}{\partial B}\right)}{LC_{bc}^2(B)C_{be}(B)C_1} - \frac{A_1\left(\dfrac{\partial C_{be}(B)}{\partial B}\right)}{LC_{bc}(B)C_{be}^2(B)C_1}\Bigg) \Bigg/ \left(\pi\sqrt{\frac{A_1}{LC_{bc}(B)C_{be}(B)C_1}}\right), \end{aligned} \tag{77}$$

where $A_1 = C_{be}(B)C_1 + C_{bc}(B)C_1 + C_{be}(B)C_{bc}(B)$.

The analytical dependences $C_{be}(B)$, $C_{bc}(B)$ and other parameters of the magnetic sensitive bipolar transistor on the magnetic field have been given in [6]. The analysis of the graph (Figure 23) shows that the highest sensitivity can be obtained with a supply voltage of 4 V. Fig. 28 shows the theoretical dependence of the sensitivity of the magnetic transducer on the basis of bipolar and FET calculated according to the expression (77). As can be seen from the graph, magnetic sensitivity is 4.5 kHz/mT.

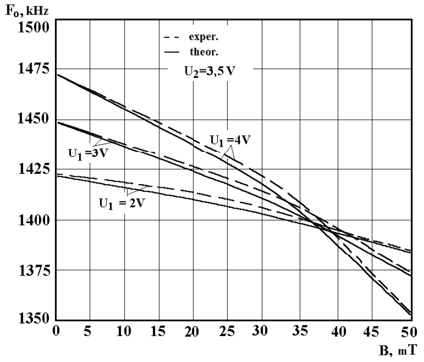

Figure 22. Theoretical and experimental dependences of generation frequency of the magnetic induction

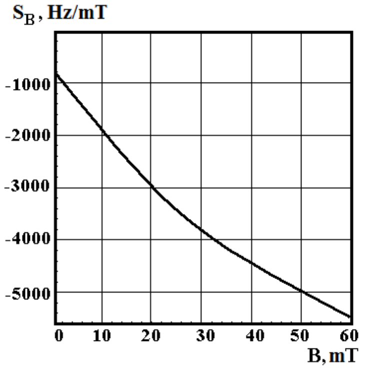

Figure 23. Theoretical dependence of the sensitivity on the magnetic induction

Let's consider the microelectronic magnetic frequency transducer on the basis of the field transistor magnetosensing device. The circuitry of the transducer is presented on fig. 24.

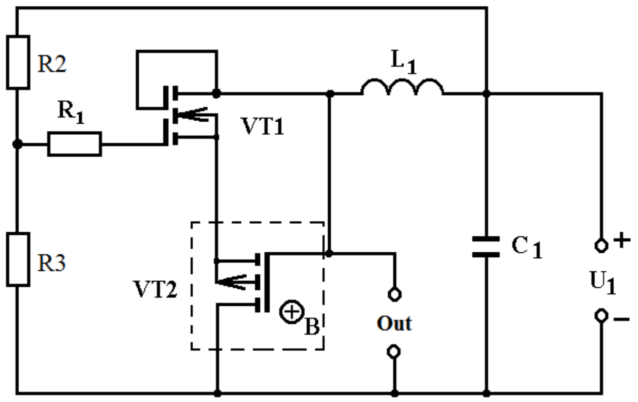

Figure 24. The electrical circuit of the magnetic transducer on the basis of the magnetosensitive field transistor

At action of cross magnetic field on the canal of transistor with the vector +B of the magnetic induction electrons on the way to the drain will deviate to subbarrier dielectric, and at action of the vector of magnetic induction in the opposite direction – deep into the volume of the semiconductor substrate. On the basis of the equivalent circuit of the transducer (fig. 24) taking into account equality to zero reactive component of output impedance at the resonance frequency, the function of transformation of the device is defined

$$F_0 = \frac{\sqrt{2}\sqrt{\dfrac{A_1 - \sqrt{A_1^2 + 4L_1C_{GD}R_{DS}^2(B)C_{GS}^2}}{L_1C_{GD}R_{DS}^2(B)C_{GS}^2}}}{4\pi}, \qquad (78)$$

where $A_1 = R_{DS}^2(B)C_{GD}C_{GS} + R_{DS}^2(B)C_{GS}^2 - L_1C_{GD}$,

Function of sensitivity of the transducer is described by expression

$$
\begin{aligned}
S_B = &-\frac{1}{8}\sqrt{2}\Big(R_{DS}^5(B)C_{GS}^5 + R_{DS}^3(B)C_{GD}^2C_{GS}\sqrt{A_2} + C_{GD}^3R_{DS}^5(B)C_{GS}^2 + C_{GD}^2R_{DS}^5(B)C_{GS}^3 + C_{GD}R_{DS}^5(B)\times \\
&\times C_{GS}^4 + C_{GD}R_{DS}^3(B)C_{GS}^3L_1 - 2C_{GD}^3R_{DS}^2(B)C_{GS}^2L_1\left(\frac{\partial R_{DS}(B)}{\partial B}\right) - 3C_{GD}^3R_{DS}^2(B)C_{GS}L_1 + 2C_{GD}^2R_{DS}^2(B)\times \\
&\times C_{GS}^3L_1\left(\frac{\partial R_{DS}(B)}{\partial B}\right) + 2C_{GD}^2R_{DS}^3(B)C_{GS}^2L_1 + R_{DS}^3(B)C_{GS}^3\sqrt{A_2} - 2\left(\frac{\partial R_{DS}(B)}{\partial B}\right)\sqrt{A_2}C_{GD}^2C_{GS}L_1 - \\
&-2R_{DS}(B)C_{GD}^2\sqrt{A_2} + 2\left(\frac{\partial R_{DS}(B)}{\partial B}\right)\sqrt{A_2}C_{GD}^3C_{GS}L_1^2 + 2C_{GD}^3C_{DS}L_1^2\Big)\Big/\Big(\pi\sqrt{A_2}L_1C_{GD}^2R_{DS}^3(B)C_{GS}^3\times \\
&\times\sqrt{-\frac{-R_{DS}^2(B)C_{GS}C_{GD} - R_{DS}^2(B)C_{GS}^2 + L_1C_{GD} - \sqrt{A_2}}{L_1C_{GD}R_{DS}^2(B)C_{GS}^2}}\Big),
\end{aligned}
\tag{79}
$$

where $A_2 = R_{DS}^4(B)C_{GS}^2C_{GD}^2 + 2R_{DS}^4(B)C_{GS}^3C_{GD} - 2R_{DS}^2(B)C_{GS}C_{GD}^2L_1 + R_{DS}^4(B)C_{GS}^4 + 2L_1R_{DS}^2(B)C_{GS}^2 + L_1^2C_{GD}^2$.

Theoretical and experimental dependences of function of transformation of device on magnetic induction are presented on fig. 25.

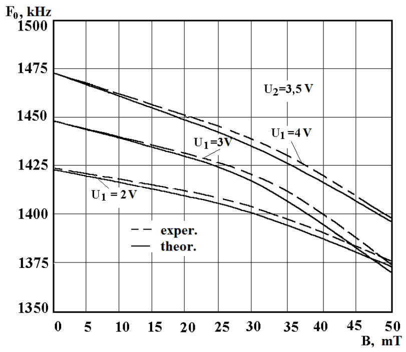

Figure 25. Theoretical and experimental dependences of function of transformation of the device on magnetic induction

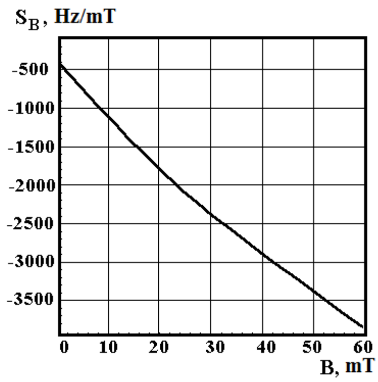

Figure 26. Dependence of sensitivity of the transducer on magnetic induction

Apparently from the schedule, the linearity of function of transformation increases with increase in supply voltage (U_1) and voltage of management (U_2). Optimum value of supply voltage and voltage of management are 4 V and 3.5 V respectively. The schedule of dependence of sensitivity of the transducer on magnetic induction is presented on fig. 26.

Functions of transformation and sensitivity were calculated by the numerical method on the personal computer according to formulas (78) and (79). The parameters of transistors necessary for calculation are taken from works [15, 16]. The sensitivity of the device at the frequency of 1418 kHz at the supply voltage of 4 V was 3 kHz/mT [21]. The adequacy of the calculated models provided in operation of devices in comparison with the experiment does not exceed ±5%.

CONCLUSION

1. The possibility of creation of microelectronic auto generator transducers of magnetic field on the basis of semiconductor devices with the negative resistance is shown that increases sensitivity, accuracy and expanding the range of measurement of magnetic field as a result of dependence of capacity, inductance and negative resistance of the tuned circuit on influence of magnetic field.
2. Theoretically and experimentally the magnetoreactive effect i.e. dependences of impedances of semiconductive diodes, bipolar and field transistors on influence of magnetic field is investigated. It is shown what active and reactive components of output impedance of these devices are changed from 10 Om/mT up to 10^3 Om/mT that creates premises for creation of frequency transducers of magnetic field.
3. Characteristics of frequency microelectronic transducers of magnetic field with such elements as magnetoresistors, magnetodiodes, magnetosensitive bipolar and field transistors, in the broad range of frequencies from 10^4 to 10^7 Hz are offered and investigated, at the same time the sensitivity of devices changes from 10^2 Hz/mT up to 10^4 Hz/mT. The developed devices allow to refuse from analog-to-digital transducers, amplifying devices at aftertreatment of information signals that increases profitability of the equipment of measurement of characteristics of magnetic field, at the same time information transfer about magnetic field on distances is possible.

BIBLIOGRAPHICAL REFERENCES

1. Microelectronic sensors of physical quantities. Edited Z. Yu. Hotra. In 3 volumes. - Lvov: League-Press, 2003. Vol.2. –595 p.
2. Baltes G. P. Integrated semiconductor sensors of magnetic field. / G.P. Baltes, R.S. Popovic//TINER.-1986, t.74, No. 8. – P.60-90.
3. Gumenyuk S. V. Integrated semiconductor magnetosensitive sensors / S.V. Gumenyuk, B.I. Podlepetsky//Foreign electronic teznika.-1989, No.12(343). –P.3-47.
4. Garyainov S.A., Abezgauz N. D. Semiconductor devices with a negative resistance. – M.: Energy, 1970, -320 p.
5. Vikulin I. M., Stafeev V.I. Semiconductor sensors. –M.: Sov. Radio, 1975. -104p.
6. Osadchuk O. V. Microelectronic frequency transducers on the basis of transistor structures with a negative resistance. – Vinnytsia. The UNIVERSUM – Vinnytsia, 2003. - 303 p.
7. Osadchuk V.S., Osadchuk A.V. The magneticreactive effect in transistors for construction transducers of magnetic field // Electronics and Electrical Engineering. – Kaunas: Technologija, 2011. –№3(109). pp.119-122.
8. Bening F. Negative resistance in electronic schemes. –M.: Soviet radio, 1975. -286p.
9. Malyshev V. A. About approximation of the volt-ampere characteristic of a tunnel interval polynoms for the quasilinear analysis of features of its work//Radio engineering and the electronic engineer.-1962, t.10, No. 9. –P 1635-1638.
10. Sidorov A. S. The theory and design of nonlinear pulse schemes on tunnel diodes. – M.: Soviet radio. 1971. - 262 p.
11. Marchenko A. N. The operated semiconductor resistors. – M.: Energy, 1978. -215 p.

12. Ladany J. An analysis of Inertial in junction Diode. // IRE Transactions on Electron Devices. -1960.ED-7, vv10.–P. 303-310.
13. Van Vliet K. M. Min H. S. Current – Voltage Relations and Equivalent Circuits of Transistors at High Injection Levels // Solid – State Electron. - 1974.–v.17.P.267-284.
14. Vikulin I. M., Stafeev V.I. Fizika of semiconductor devices. – M.: Radio and communication. 1990. - 264 p.
15. PSPICE Users guide / MicroSim Corporation La Cadena Drive, Laduna Hills.1989. - 450 p.
16. Razevig V. D. Application of the Z-SAD and Pspise program for circuitry modeling on PEVM. Release 3. Modeling of analog devices / EL of Razevig. – M.: Radio and communication. 1992. –120 p.
17. Osadchuk A.V., Osadchuk V.S. Radiomeasuring Microelectronic Transducers of Physical Quantities // Proceedings of the International Siberian Conference on Control and Communications (SIBCON). 21-23 May 2015. Omsk. 978-1-4799-7103-9/15.
18. Potemkin V. G. The system of engineering and scientific calculations Matlab 5.x in two volumes. T.1 / V.G. Potemkin. – M.: Dialogue – MIFN, 1999. - 260 p.
19. Osadchuk V. S The Microelectronic Radiomeasurind Transducers of Magnetic Field with Frequency Output. / V. S. Osadchuk, A. V. Osadchuk// Electronics and Electrical Engineering.. – Kaunas: Techolodija.– 2011.–№4 (110). – P.67-70.
20. Osadchuk A. V., Osadchuk V. S. Frequency Magnetic Transducers on Base of Bipolar Transistors Structure. Conference Proceedings. 2017 IEEE 37 International Conference on Electronics and Nanotechnolody (ELNANO) April 18-20.2017 Kyiv, Ukraine. –P.156-161.
21. Osadchuk V. S., Osadchuk A. V. Radiomeasurement Transducer to Magnetic Induction with Frequency Output// The International Conference “Modern Problems of Radio Engineering, Telecommunication and Computer Science” TCSET 2006, Lviv–Slavske, 2006, –P.490-492.

The Potential of Modern Science
volume 3

Editor: Babych Mykola Mykolayovich
Published by Sciemcee Publishing.
LP22772, 20-22 Wenlock Road
London, United Kingdom
N1 7GU
Sciemcee Publishing is part of SCIEMCEE.
It furthers the SCIEMCEE's mission by disseminating knowledge in the pursuit of education, learning and research at the highest international levels of excellence.

First Edition: 2019

A catalogue record for this publication is available from British Library.

ISBN 978-1-9993071-3-4
Includes bibliographical references and index.

SCIEMCEE
PUBLISHING LONDON